Arch Microbiol (2009) 191:797–806
DOI 10.1007/s00203-009-0511-x

ORIGINAL PAPER

Lysine-91 of the tetraheme *c*-type cytochrome CymA is essential for quinone interaction and arsenate respiration in *Shewanella* sp. strain ANA-3

Kamrun Zargar · Chad W. Saltikov

Received: 17 June 2009 / Revised: 24 August 2009 / Accepted: 2 September 2009 / Published online: 17 September 2009

Abstract The tetraheme *c*-type cytochrome, CymA, is essential for arsenate respiratory reduction in *Shewanella* sp. ANA-3, a model arsenate reducer. CymA is predicted to mediate electron transfer from quinols to the arsenate respiratory reductase (ArrAB). Here, we present biochemical and physiological evidence that CymA interacts with menaquinol (MQH_2) substrates. Fluorescence quench titration with the MQH_2 analog, 2-*n*-heptyl-4-hydroxyquinoline-*N*-oxide (HOQNO), was used to demonstrate quinol binding of *E. coli* cytoplasmic membranes enriched with various forms of CymA. Wild-type CymA bound HOQNO with a K_d of 0.1–1 μM. It was also shown that the redox active MQH_2 analog, 2,3-dimethoxy-1,4-naphthoquinone ($DMNH_2$), could reduce CymA in cytoplasmic membrane preparations. Based on a CymA homology model made from the NrfH tetraheme cytochrome structure, it was predicted that Lys91 would be involved in CymA-quinol interactions. CymA with a K91Q substitution showed little interaction with HOQNO. In addition, $DMNH_2$-dependent reduction of CymA-K91Q was diminished by 45% compared to wild-type CymA. A Δ*cymA* ANA-3 strain containing a plasmid copy of *cymA*-K91Q failed to grow with arsenate as an electron acceptor. These results suggest that Lys91 is physiologically important for arsenate respiration and support the hypothesis that CymA interacts with menaquinol resulting in the reduction of the cytochrome.

Keywords Tetraheme cytochrome · Shewanella · Quinone · Arsenate reduction

Communicated by Wolfgang Buckel.

Electronic supplementary material The online version of this article (doi:10.1007/s00203-009-0511-x) contains supplementary material, which is available to authorized users.

K. Zargar · C. W. Saltikov (✉)
Department of Microbiology and Environmental Toxicology, University of California, 1156 High Street, Santa Cruz, CA 95064, USA
e-mail: saltikov@metx.ucsc.edu

Introduction

Arsenic is naturally occurring in various environments, from hypersaline lakes to aquifers used for drinking water and agriculture. Although many factors contribute to the presence of arsenic in water, respiratory arsenate reduction is thought to play a critical role in arsenic accumulation in anaerobic groundwater [Reviewed in (Oremland and Stolz 2003; Reyes et al. 2008)]. *Shewanella* sp. ANA-3 is a model arsenate respiratory reducer that has been used in several geochemical studies aimed at understanding how arsenic is mobilized from iron oxides and into solution (Campbell et al. 2006; Tufano et al. 2008). Moreover, ANA-3 has also been used to investigate the genetic and biochemical mechanisms for anaerobic respiration of arsenate (Saltikov and Newman 2003; Saltikov et al. 2005; Murphy and Saltikov 2007). Two genes, *arrA* and *arrB*, are known to be essential for anaerobic growth on arsenate and its reduction to arsenite. ArrA is a ~95 kDa molybdenum-containing arsenate reductase, and ArrB is a ~26 kDa Fe–S containing protein that interacts with ArrA. In 1997, Myers and Myers cloned and sequenced the *cymA* gene from *Shewanella oneidensis* MR-1 and showed that it was necessary for anaerobic respiration on Fe(III), nitrate, Mn(IV), and fumarate (Myers and Myers 1997). Recently, *cymA*, was also shown to be critical for anaerobic arsenate respiration (Murphy and Saltikov 2007). CymA is a 21 kDa cytoplasmic membrane bound tetraheme *c*-type

cytochrome that is predicted to mediate electron transfer from reduced quinones to downstream electron transport components such as the periplasmic arsenate respiratory reductase (ArrAB) (Oremland and Stolz 2003; Saltikov and Newman 2003).

The goal of this study was to investigate the interactions between CymA and menaquinols (MQH_2) and determine how these interactions impact arsenate respiration in *Shewanella* sp. ANA-3. We used biochemical and genetic approaches to characterize the MQH_2-CymA interactions. Multiple sequence alignments of NrfH (tetraheme *c*-type cytochrome of nitrite reductase complex), NapC (tetraheme *c*-type cytochrome of nitrate reductase complex), and CymA, and homology modeling of CymA with the NrfAH crystal structure were also used to identify amino acid residues in CymA that might be important for MQH_2 interactions and growth on arsenate.

Materials and methods

Bacterial strains and plasmids

Strains and plasmids used in this study are listed in Table 1. The pBAD-TOPO TA expression kit (Invitrogen, CA) was used to over-express CymA. The *cymA* gene without the stop codon was cloned into the pBAD-TOPO TA vector and verified by DNA sequencing. The pBAD-*cymA* plasmid was co-transformed with pEC86, containing *E. coli ccm* genes, into *E. coli* TOP10 cells. The pBAD-*cymA* plasmid was used to generate point mutations by site-directed mutagenesis as described later. We generated CymA point mutations used in growth curve studies using the CymA complementation vector pAN-*cymA* (Murphy and Saltikov 2007). pAN*cymA*-v5-his was created by using the pBAD forward and reverse primers to generate a *cymA*-v5-his PCR product. The PCR product was then ligated into pBBR1-MCS2 to generate pAN*cymA*-v5-his.

Preparation of CymA-enriched cytoplasmic membranes of *E. coli*

A freshly transformed *E. coli* expression strain was grown in 1 L cultures (LB/Ampicillin 100 μg/mL) at 37°C and induced with 0.02% arabinose when the OD 600 nm of 0.6 was reached. After 16 h of induction at 28°C, cells were harvested and lysed by sonication in ice-cold MOPS buffer (100 mM MOPS/KOH and 5 mM EDTA, pH 7.0, 0.2 mM protease inhibitor AEBSF hydrochloride). Unbroken cells were removed by centrifugation. Crude membranes were

Table 1 Bacterial strains and plasmids used in this study

Strain or plasmid	Genotype or markers, characteristics, and uses	Source or references
E. coli strains		
TOPO Top 10	*E. coli* host for expression; F^- *mcrA* Δ(*mrr-hsdRMS-mcrBC*) φ80*lacZ*ΔM15 Δ*lacX74 recA1 araD139* Δ(*ara-leu*)*7697 galU galK rpsL* (Str^r) *endA1 nupG*	Invitrogen
DH5α	F^- *endA*1 *glnV*44 *thi*-1 *recA*1 *relA*1 *gyrA*96 *deoR nupG* Φ80d*lacZ*ΔM15 Δ(*lacZYA-argF*)U169, *hsdR*17(r_K^- m_K^+), *λ*–	(Saltikov and Newman 2003)
BL21(DE3)	F^- *ompT gal dcm lon hsdS*$_B$(r_B^- m_B^-) *λ*(DE3 [*lacI lacUV*5-T7 gene 1 *ind*1 *sam*7 *nin*5])	Professor Karen Ottemann, UCSC
WM3064	Donor strain for conjugation; *thrB*1004 *pro thi rpsL hsdS lacZ*ΔM15 RP4-1360 Δ(*araBAD*)*567 ΔdapA*1341::[*erm pir*(wt)]	W. Metcalf, Univ. Illinois; (Saltikov and Newman 2003)
Shewanella strains		
Shewanella sp. ANA-3	Isolated from an As-treated wooden pier piling in a brackish estuary (Eel Pond, Woods Hole, MA)	(Saltikov et al. 2003)
AN-CYMA	*Shewanella* sp. strain ANA-3; Δ*cymA*; does not respire As(V) or fumarate	(Murphy and Saltikov 2007)
Plasmids/Vectors		
pBBR1-MCS2	5.1 kb broad-host range plasmid used for complementation: Km^r, *lacZ*	(Kovach et al. 1994)
pAN*cymA-v5-his*	5.1 kb broad-host range plasmid used for complementation: Km^r, *lacZ* with *cymA-v5-6x his* insert	This study
pBAD-TOPO-TA	4.1 kb expression vector; *araC*, V5 epitope, 6x His; Amp^r	Invitrogen
pBAD-*cymA*	pBAD-TOPO-TA with *cymA* insert	This study
pBAD-*cymA*-K91Q	pBAD-TOPO-TA with *cymA* K91Q insert	This study
pEC86	Expression vector harboring *E. coli ccmABCDEFGH*, Cm^r	(Thony-Meyer et al. 1995)
pAN*cymA*	ANA-3 *cymA* complementation vector; Km^r	(Murphy and Saltikov 2007)
pAN-*cymA*-K91Q	ANA-3 *cymA* complementation vector with K91Q mutation; Km^r	This study
pAN-*cymA*-K90Q	ANA-3 *cymA* complementation vector with K90Q mutation; Km^r	This study

prepared by differential centrifugation at 150,000*g* for 1.5 h at 4°C. Cytoplasmic membranes were obtained by layering the crude membranes on top of 55% (W/V) sucrose followed by ultracentrifugation at 150,000*g* for 1.5 h at 4°C. The red floating band of cytoplasmic membranes enriched with CymA was removed and further purified by repeated ultracentrifugation and resuspension of the pellet in MOPS buffer. The final CymA-enriched cytoplasmic membranes were resuspended in MOPS buffer and flash frozen in liquid nitrogen and stored at −70°C until further use (Rothery et al. 2005). The heme concentration was estimated by pyridine hemochrome assay as previously described (Berry and Trumpower 1987).

SDS–PAGE and heme staining

SDS–PAGE (29:1 30% acrylamide) was used to analyze protein extracts. Gels contained 18% polyacrylamide. In-gel heme staining was done as previously described (Francis and Becker 1984). Briefly, 0.2 g of *o*-dianisidine was dissolved in 20 mL of glacial acetic acid then added to 160 mL of deionized H_2O. While dissolving the *o*-dianisidine, the SDS–PAGE gel was washed in 200 mL 12.5% TCA (trichloroacetic acid) for 30 min. The TCA wash was followed by a 30 min wash in deionized H_2O. As the gel was being washed, 20 mL of 0.5 M sodium citrate buffer (pH 4.4) and 0.4 mL of 30% hydrogen peroxide were added to the *o*-dianisidine solution. The solution was poured over the gel while shaking until bands appeared.

Western blot

Western blot was performed as follows. The SDS–PAGE gel was transferred to PVDF membrane over night at 4°C and a constant 30 V. After the transfer, membranes were blocked with TBS (tris buffered saline), 5% NFDM (non-fat dry milk), and 0.1% Tween-20 for 2 h. Following the blocking, the membrane was soaked in TBS, 5% NFDM, 0.1% Tween-20 with anti-V5-HRP at 1:5,000 dilution overnight at 4°C while shaking. The next morning the blot was washed 6 × 5 min with TBS 0.1% Tween-20 followed by one 20 min wash with deionized H_2O. The blots were developed using ECL + Plus western blotting system (Cat# RPN 2132) from Amersham.

Fluorescence quench titration (FQT) with HOQNO

The interaction of CymA-enriched membranes with the MQH_2 analog 2-*n*-heptyl-4-hydroxyquinoline-*N*-oxide (HOQNO) (Alexis Corp) was determined using FQT as previously described (Rothery et al. 2005). The Perkin Elmer LS-50B fluorescence spectrometer was used to monitor fluorescence intensities of HOQNO with excitation and emissions wavelengths of 341 and 479 nm, respectively. All experiments were performed at room temperature (25°C) and pH 7.0 in 100 mM MOPS/KOH and 5 mM EDTA. HOQNO was incrementally added to a stirred quartz cuvette prepared in a 100 μM ethanolic solution. Protein concentrations of 0.1, 0.2, 0.3, and 0.4 mg ml^{-1} were used for each FQT experiment. The disassociation constant, K_d, was determined using an equation (Eq. 1) that describes the fluorescence (F) of a ligand binding to an enzyme at a site as described previously (Rothery et al. 2005). The equation, variable, and calculation of K_d are summarized below:

$$F_{obs} = (f_{bound} - f_{free}) \times \left\{ Q - \sqrt{Q^2 - n_s[E_{tot}] \times [I_{tot}]} \right\} + f_{free} \times [I_{tot}] \quad (1)$$

$$Q = 1/2 \times ([I_{tot}] + K_d + n_s \times [E_{tot}]) \quad (2)$$

$$[I_{tot}] = [I_{bound}] + [I_{free}] \quad (3)$$

The specific fluorescence (F μM^{-1}) of free (f_{free}) HOQNO is determined from the linear increase in fluorescence following the FQT point. Specific fluorescence of bound HOQNO (f_{bound}) is assumed to be zero. The concentrations (μM) of total, bound, and free inhibitor (e.g., HOQNO) correspond to $[I_{tot}]$, $[I_{bound}]$, and $[I_{free}]$, respectively. The number of HOQNO binding sites and total enzyme concentrations correspond to n_s and $[E_{tot}]$, respectively. It was assumed that one molecule of HOQNO binds to one CymA molecule. The CymA concentration ($[E_{tot}]$) was calculated from the molar extinction coefficient of reduced minus oxidized spectra of a single *c*-type heme assumed to be ~21.84 mM^{-1} cm^{-1} at 552 nm, using UV/VIS spectroscopy (Berry and Trumpower 1987; Rothery et al. 2005). Lastly, K_d was calculated using known variables ($[E_{tot}]$, n_s, f_{free}, $[I_{tot}]$) for F_{obs} corresponding to HOQNO at particular FQT points as described in the "Results" section.

$DMNH_2$ mediated reduction of CymA

$DMNH_2$ reduction of CymA-enriched cytoplasmic membranes was observed by UV/VIS spectrophotometric approach. The following manipulations were done in an anaerobic glove box (N_2 96%, H_2 4%). An anaerobic 1 ml reaction was prepared in buffer [100 mM MOPS/KOH and 5 mM EDTA (pH 7.0)] and *E. coli* cytoplasmic membrane enriched with CymA. DMN was prepared as a 10 mM methanolic stock solution and reduced to $DMNH_2$ with a 50 mM $NaBH_4$ stock made in water with 0.6% NaOH. The final reaction contained 10 μM $DMNH_2$. Dithionite was freshly prepared in 50 mM Tris pH 10.0 at a concentration of 500 mM. The anaerobic cuvette was plugged with a

butyl rubber stopper, removed from the glove box, and immediately analyzed in the spectrophotometer (Beckman, DU650).

Shewanella growth curve analysis

Standard culturing of *Shewanella* sp. ANA-3 was performed in Luria–Bertani (LB) medium or a semi-defined medium referred to as TME (Murphy and Saltikov 2007) consisting of 1.5 g L^{-1} NH_4Cl, 0.6 g L^{-1} $NaHPO_4$, 0.1 g L^{-1} KCl, 0.5 g L^{-1} yeast extract, 10 mM HEPES, 20 mM lactate, and 10 ml L^{-1} (each) trace mineral and vitamin solutions (Murphy and Saltikov 2007). Anaerobic medium was prepared by boiling under a stream of N_2 and anaerobically dispensing into N_2-flushed Balch tubes that were sealed with butyl rubber stoppers and autoclave sterilized. Media were supplemented with 10 mM arsenate (pH 7) from sterile anaerobic stock solutions. *Shewanella* sp. ANA-3 strains were grown at 30°C, and aerobic liquid cultures were shaken at 250 rpm. Growth curves were initiated from aerobically grown cultures prepared in TME media. Various strains were inoculated into anaerobic Balch tubes at similar densities. Growth was monitored over time by measuring the $OD_{600\ nm}$ with a Spectronic 20D+.

Mutagenesis

Mutations to Lys90 and Lys91 of ANA-3 *cymA* were generated based on the QuickChange Site-Directed Mutagenesis method (Stratagene). Primers AN-CymA-K90Q-F (5′- GGT CCA GTG GAT TAC TTG ATT cag AAA ATC ATC G-3′), AN-CymA-K90Q-R (5′-C GAT GAT TTT ctg AAT CAA GTA ATC CAC TGG ACC-3′), AN-CymA-K91Q-F (5′- CCA GTG GAT TAC TTG ATT AAG caa ATC ATC GTA TCT AAA GAC- 3′), and CymA-K91Q-R (5′-GTC TTT AGA TAC GAT GAT ttg CTT AAT CAA GTA ATC CAC TGG-3′) were designed with a lysine to glutamine substitution (in lowercase). The *cymA* mutagenesis reaction consisted of a 25 μL mixture containing 2.5 μL 10× *Pfu*-Turbo Hotstart Buffer (Strategene), 0.2 mM deoxynucleoside triphosphate mix, 125 ng primer, 50 ng pAN*cymA* plasmid, 1 μL *Pfu*-Turbo Hotstart DNA polymerase (Stratagene), and nuclease-free water. Samples were incubated with the following thermocycle profile: 95°C for 30 s and 18 cycles of 95°C for 30 s, 55°C for 1 min, and 68°C for 11 min. The reaction mixtures were cooled to room temperature, and 1 μL *Dpn*I (10 units) was added to each reaction mixture and incubated for 1 h at 37°C. Each reaction mixture was transformed into a DH5α strain. Plasmids were extracted and sequenced to confirm the correct mutation. The resulting K90Q- and K91Q-mutated pAN*cymA* vectors were then transformed into AN-CYMA by conjugation as previously described (Saltikov and Newman 2003). The plasmid strains were denoted pAN-*cymA*-K90Q and pAN-*cymA*-K91Q, for mutations to Lys90 and Lys91, respectively.

Multiple sequence alignment and homology modeling of CymA

Multiple sequence alignment of *Shewanella* sp. ANA-3 CymA, *E. coli* NapC, and *Desulfovibrio vulgaris* NrfH were performed using ClustalW (Thompson 1994). PSI-PRED was used to predict the secondary structure of CymA (Jones 1999). The homology model of CymA based on *D. vulgaris* NrfAH crystal structure was created using SWISS-MODEL (Arnold et al. 2006).

Results

Expression of CymA in *E. coli*

We used the pBAD-TOPO TA expression plasmid (Invitrogen) to over-express CymA in *E. coli*. This plasmid features an L-arabinose inducible promoter, a V5 epitope, and 6× His-tag fused to the C-terminus of the expressed protein. Previous studies have shown that over-expression of multiheme *c*-type cytochromes in *E. coli* required simultaneous over-expression of cytochrome maturation genes (Thony-Meyer et al. 1995). CymA-enriched membranes were prepared in an *E. coli* host co-transformed with pBAD*cymA* (and *cymA* alleles) and pEC86; the latter plasmid constitutively expresses the *E. coli* cytochrome maturation genes. Based on the hemochrome pyridine analysis, 1 mg mL^{-1} of cytoplasmic membrane yielded 12.5 μM of CymA. While 0.1 μg of cytoplasmic membrane preparation was sufficient for western blot detection of CymA (wild-type and *cymA* alleles), 10 μg was needed to detect CymA expressed without hemes (in *E. coli* lacking the *ccm* plasmid). We speculated that this was due to degradation of CymA apo-protein. Heme staining confirmed the lack of heme detection in extracts prepared from *E. coli* without pEC86 (Fig. 1). These results are consistent with previous work showing that an *E. coli* Δ*ccmABCDEFGH* mutant failed to synthesize mature cytochrome *c* (Thony-Meyer et al. 1995). Furthermore, we showed that CymA fused to the V5 epitope, and the 6× His-tag (pAN*cymA*-v5-his) was capable of complementing the growth of ANA-3 Δ*cymA* strain on arsenate (Fig. S1A), indicating that the modified CymA protein still functions normally in respiratory arsenate reduction. CymA-K91Q-enriched membranes were expressed, purified, and stored similar to wild type.

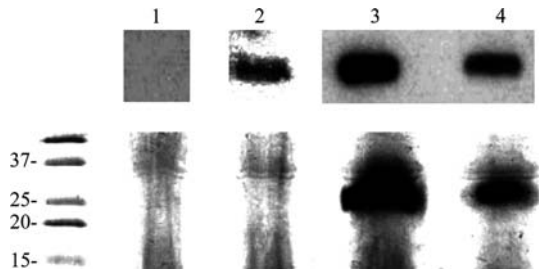

Fig. 1 CymA expression. *Top panel* western blot analysis. *Bottom panel* heme stain. Lanes correspond to *1*, membrane only; *2*, CymA − *ccm*; *3*, CymA + *ccm*.; and *4*, CymA K91Q + *ccm*. All samples are cytoplasmic membrane fractions. The western blot analysis contained 0.1 μg protein per lane, except for CymA − *ccm*, which contained 10 μg of protein. All heme stain samples were loaded at 50 μg of protein per lane

Homology model of CymA and prediction of key amino acids

To predict a homology model of CymA, ClustalW was first used to perform a multiple sequence alignment of the primary amino acid sequence of *E. coli* NapC, the tetraheme subunit of nitrate reductase (EcNapC), *Desulfovibrio vulgaris* NrfH, the tetraheme subunit of nitrite reductase (DvNrfH), and CymA (ANA3CYMA) (Fig. 2a) (Thompson et al. 1994). PSIPRED was then used to predict the secondary structure of CymA, which is presented above the alignment (Fig. 2a). Finally, Swiss-Model was used to predict a homology model of CymA based on the structure of DvNrfAH (PDB ID: 2J7A), nitrite reductase (Fig. 2b) (Arnold et al. 2006). Using the multiple sequence alignments, homology model (Fig. 2), and other reports, we predicted that Lys91 of CymA would be important for interacting with menaquinol-like substrates (Rodrigues et al. 2006). Lys91 is located in the putative second helix of CymA, which is proposed to interface with the cytoplasmic membrane and periplasmic space (Fig. 2b) (Rodrigues et al. 2006).

HOQNO interactions with CymA-enriched membranes

MQH_2-CymA interactions were investigated indirectly by fluorescence quench titration (FQT) with HOQNO, a fluorescent MQH_2 structural analog. FQT with HOQNO has been used to characterize quinol binding to membrane subunits of the fumarate and DMSO reductases (Rothery and Weiner 1996; Rothery et al. 2005). When titrating HOQNO into a sample containing an interacting partner, fluorescence quenching should be observed until all the binding sites become saturated. After the fluorescence quench titration point, continued HOQNO additions typically yield a linear increase in fluorescence reflecting free HOQNO. When applying FQT to CymA-enriched cytoplasmic membranes, compared to membranes without CymA (Fig. 3a), we observed dramatic fluorescent quenching with membranes enriched with CymA (Fig. 3b). Using Eqs. 1–3 (Rothery et al. 2005), we estimated the HOQNO disassociation constant (K_d,) for CymA to be 0.1–1.0 μM. We could not determine whether CymA over-expressed without pEC86 interacted with HOQNO because of the low CymA content in these membrane preparations (100 fold less than membranes expressed with pEC86).

The role of CymA Lys91 in HOQNO interactions

To investigate the role of Lys91, we substituted this site with Gln (K91Q) and over-expressed the mutant allele (called *cymA*-K91Q) in *E. coli*. FQT response (Fig. 3c) for CymA-K91Q was linear indicating weak interactions with HOQNO. A representative western and in-gel heme stain of cytoplasmic membranes enriched with CymA-K91Q are shown in Fig. 1. Semi-quantitative western blot with densitometry showed that the CymA-K91Q expression in the membrane preparation was ~75% of those containing wild-type CymA (data not shown). Because the CymA-K91Q expression was ~25% less than that of the wild type, the decreased HOQNO quenching that was observed in Fig. 3c could be due to less CymA and not the mutation. A closer inspection of the 0–0.5 μM HOQNO FQT curves of wild-type CymA and CymA-K91Q (Fig. 3d) showed a linear increase in fluorescence (and no quenching) with CymA-K91Q-enriched membranes for 0.2 mg mL^{-1} and 0.3 mg mL^{-1} protein concentrations. In contrast, significant fluorescence quenching compared to CymA-K91Q was observed for wild-type CymA-enriched membranes. Moreover, fluorescence quenching of the wild-type CymA increased with increasing protein concentration unlike CymA-K91Q. This comparison indicated that the decreased HOQNO quenching in CymA-K91Q is most likely due to the amino acid substitution and not due to the 25% decrease in protein expression relative to the wild type. Based on these observations, we concluded that substituting Lys91 with an uncharged amino acid such as Gln disrupted quinol interactions.

Reduction of CymA with $DMNH_2$

We were interested in determining whether CymA interactions with MQH_2 substrates could lead to heme reduction. This was investigated by using $DMNH_2$, a redox active structural analog of menaquinol, as a relevant physiological reductant for CymA. For cytochromes like CymA, their oxidation and reduction can be monitored in membrane preparations by observing redox-induced changes in specific absorption peaks such as the Soret band (410 nm shifts to 420 nm) and the appearance of α-

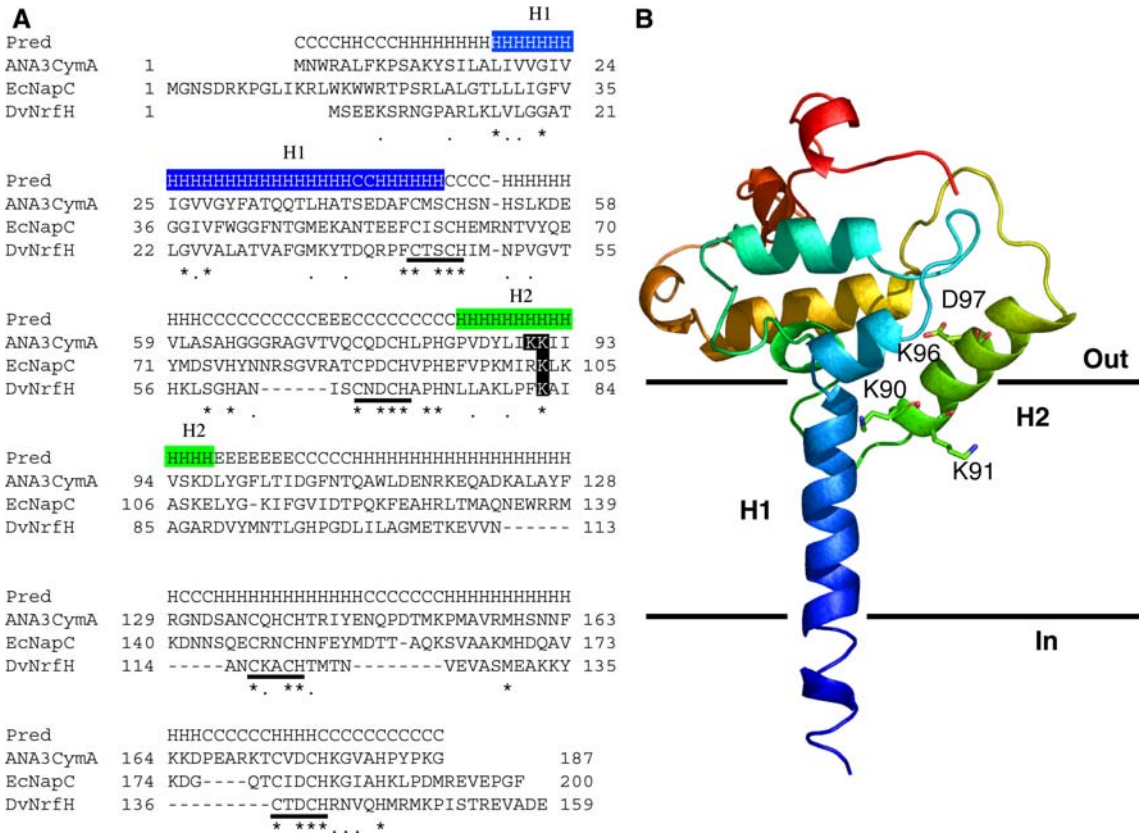

Fig. 2 NapC, NrfH, and CymA multisequence alignment and homology model of CymA to DvNrfH, tetraheme cytochrome subunit of nitrite reductase NrfAH. **a** The primary amino acid sequences of *Shewanella* sp. ANA-3 CymA (AnaCymA, Shewana3_3977, Genbank accession YP_871601), *E. coli* nitrate reductase (EcNapC, Genbank accession NP_416706), and *Desulfovibrio vulgaris* nitrite reductase (DvNrfH, Genbank accession YP_009846) were aligned using ClustalW. PSIPRED (http://bioinf.cs.ucl.ac.uk/psipred/psiform.html) was used to predict CymA secondary structure, which is presented above the alignment (Pred); *C*, *H*, and *E* indicate coil, helix, and strand, respectively. *Helix 1* and *2* are indicated above the alignment by *H1* and *H2*, respectively. The Lys residues involved in putative menaquinol binding and oxidation are highlighted with *black boxes*. The *c*-type heme binding motifs, CXXCH, are *underlined*. **b** Homology model of CymA and highlighted residues predicted to be involved in CymA-menaquinol interaction and MQH_2 oxidation. *H1* and *H2* indicate the first and second helix of CymA, respectively. Swiss Modeler was used to predict the structure of CymA using DvNrfAH (PDB ID: 2J7A) as a template

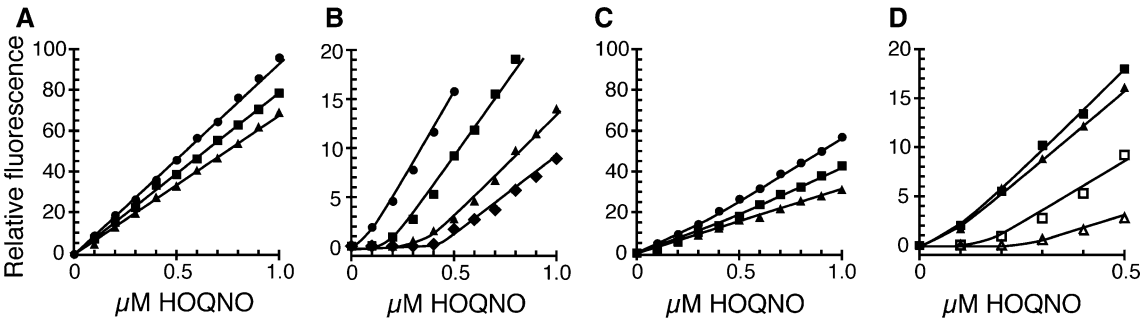

Fig. 3 Fluorescence quench titration (FQT) of *E. coli* cytoplasmic membrane fractions. The experiment was performed at room temperature, and HOQNO was added from a 10 mM ethanolic solution. **a** Membrane only **b** CymA + *ccm* **c** CymA K91Q + *ccm*, and **d** comparison of (*filled square*) 0.2 mg mL^{-1} and (*filled triangle*) 0.3 mg mL^{-1} FQT curves of CymA K91Q + *ccm* and (*open square*) 0.2 mg mL^{-1} and (*open triangle*) 0.3 mg mL^{-1} wild-type CymA + *ccm*. Each sample was assayed at three different protein concentrations: (*filled circle*) 0.1 mg mL^{-1}, (*filled square*) 0.2 mg mL^{-1}, and (*filled triangle*) 0.3 mg ml^{-1}. CymA + *ccm* was further assayed at (*filled diamond*) 0.4 mg mL^{-1}. 1 mg ml^{-1} of cytoplasmic membranes corresponded to 12.5 μM CymA. Plots are representatives of three independent FQT experiments. Note that the *Y*-axis scale changes in *panel A through D*

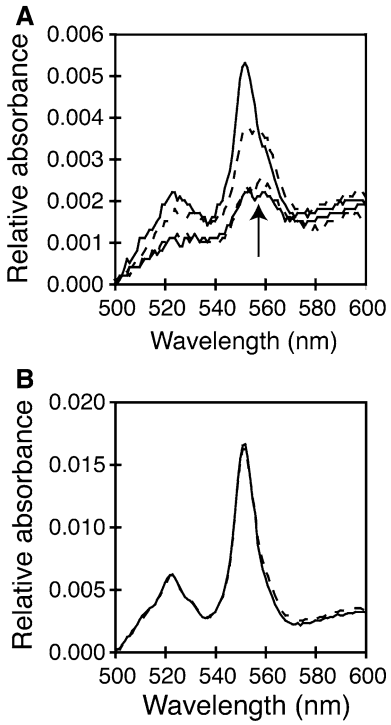

Fig. 4 Reduced minus air-oxidized spectra of *E. coli* cytoplasmic membrane enriched with CymA (*solid curves*) or CymA-K91Q (*dashed curves*). **a** The *two larger peaks* represent the membranes reduced with $DMNH_2$. The *two smaller peaks* (indicated by an *arrow*) represent membranes reduced with only $NaBH_4$. **b** Dithionite-reduced membranes. The spectra are representative spectra from three different experiments

(552 nm) and β-bands (525 nm). Figure 4 shows difference spectra of air-oxidized minus reduced CymA-enriched cytoplasmic membranes with several different reductants: $NaBH_4$, $DMNH_2$ (DMN reduced with $NaBH_4$), and sodium dithionite; all three could reduce CymA, however, with dramatically varying degrees of efficiency. Membranes without CymA reduced with $DMNH_2$, dithionite, and $NaBH_4$ showed no noticeable changes in Soret, α-, and β-bands (data not shown). Table 2 shows the estimated amount of heme reduced with the three different reductants. Dithionite alone reduced the most heme, $\sim$655 pmol compared to $DMNH_2$ (165 pmol) (Table 2). The same amount of $NaBH_4$ used in preparing the $DMNH_2$ stock reduced only $\sim$32 pmol heme. The greater reduction of CymA by dithionite relative to $DMNH_2$ is likely due to differences in their redox potentials [-660 and -75 mV, respectively (Lancaster et al. 2000)] and how these reductants interact with CymA. Dithionite is predicted to directly reduce the heme groups of CymA. However, $DMNH_2$-dependent reduction of CymA most likely occurs at the Q-site, which is located in helix 2 (Fig. 2). Moreover, $DMNH_2$ lacks a lipophilic carbon tail (unlike endogenous menaquinols). These factors likely led to the decreased efficiency of $DMNH_2$-dependent reduction of CymA relative to dithionite. Despite these observations, we concluded that CymA could be reduced by a redox active MQH_2 analog.

$DMNH_2$-dependent reduction of CymA-K91Q

Cytoplasmic membranes enriched with CymA-K91Q showed similar reduction patterns with dithionite (627 pmol) and $NaBH_4$ (37 pmol) (Table 2). However, $DMNH_2$-dependent heme reduction was diminished by 50% (87 pmol) in CymA-K91Q-enriched cytoplasmic membranes compared to those of wild-type CymA (165 pmol). These reactions were carried out with similar heme content determined through pyridine hemochrome analysis. Moreover, the dithionite-reduced spectra of cytoplasmic membrane preparations for both CymA and CymA-K91Q were indistinguishable (Fig. 4b) also suggesting that the heme content in both reactions was the same and could be reduced by the same amount. Therefore, the diminished 552 nm absorption peak for $DMNH_2$-reduced CymA-K91Q (Fig. 4a) is most likely attributed to the alterations in MQH_2 binding site of CymA-K91Q. Lys91 is likely to be important for MQH_2-dependent reduction of CymA.

Physiology of CymA Q-site mutations in *Shewanella* sp. ANA-3

Though we have shown that *E. coli* cytoplasmic membrane fractions expressing CymA-K91Q did not quench HOQNO fluorescence and had diminished capabilities of being reduced with $DMNH_2$, we wanted to investigate the physiological effects of the *cymA*-K91Q allele in *Shewanella* sp. ANA-3 Δ*cymA* strain. From an earlier investigation of the role of *cymA* in arsenate respiration, we could complement a Δ*cymA* strain with a plasmid containing the wild-type *cymA* allele (pAN-*cymA*) (Murphy and Saltikov 2007). Using pAN-*cymA* as a template for site-directed mutagenesis, we introduced K91Q into *cymA* to generate the plasmid pAN-*cymA*-K91Q. Anaerobic arsenate growth curves were generated with *Shewanella* sp. ANA-3 Δ*cymA* strains harboring the pAN-*cymA* or pAN-*cymA*-K91Q plasmids (Fig. 5). The *cymA*-K91Q allele failed to complement the Δ*cymA* strain grown on arsenate. Furthermore, the *cymA*-K91Q allele also failed to complement the Δ*cymA* strain when grown on fumarate (Fig. S1B) and on Fe(III) citrate (data not shown). In addition to K91Q, we also considered Lys90 because of its close proximity to Lys91 (Fig. 2). A *Shewanella* sp. ANA-3 Δ*cymA* strain with *cymA*-K90Q allele was generated from pAN-*cymA*. Unlike K91Q, the *cymA*-K90Q allele was able to complement the Δ*cymA* ANA-3 strain similar to wild type (data

Table 2 Physiology and menaquinol-binding properties of CymA

Strain	Growth on As(V)[a]	Dithionite heme reduction (pmol)	$NaBH_4$ heme reduction (pmol)	$DMNH_2$ heme reduction (pmol)	K_d (μM)
Wild type	+	655	32	165	0.1–1.0
K91Q	−	627	37	87	−
K90Q	+	ND	ND	ND	ND

ND Not determined

[a] + and − refer to growth or no growth, respectively

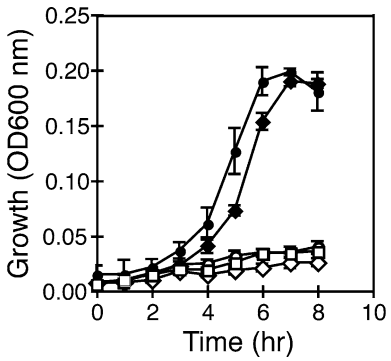

Fig. 5 Growth curve analysis of *Shewanella* sp. strain ANA-3 grown anaerobically with 20 mM lactate and 10 mM arsenate. Symbols represent: *filled circle* wild type, *open circle* Δ*cymA*, *open square* Δ*cymA* with vector pBBR1-MCS2, *filled diamond* Δ*cymA* with complementation vector pAN-*cymA*, and *open diamond* Δ*cymA* with complementation vector pAN-*cymA*-K91Q. *Data points* and *error bars* represent averages and standard deviations of triplicate cultures, respectively

not shown). This result suggests that Lys90 may not be important in menaquinol interaction, unlike Lys91.

Discussion

The aim of this study was to investigate the interactions between CymA and MQH_2 in arsenate respiration. To investigate this interaction, we used MQH_2 structural analogs 2-*n*-heptyl-4-hydroxyquinoline-*N*-oxide (HOQNO) and the redox active analog 2,3-dimethoxy-1,4-naphthoquinone(ol) ($DMN(H_2)$). Although HOQNO is a well-known respiratory inhibitor, the use of FQT with HOQNO has not been applied before to understanding quinone interactions with NapC/NrfH-like tetraheme cytochromes. Using this technique, we showed that *E. coli* membranes enriched in CymA interacted with HOQNO with an estimated K_d of 0.1–1 μM. In membranes lacking CymA, we observed a linear increase in fluorescence of HOQNO (Fig. 3a), indicating that HOQNO interaction with endogenous partners in the membranes was weak or minimal. From this observation, we concluded that the increased quenching observed in Fig. 3b is due to the presence of CymA in the membrane. In comparison, Brandt and Jagow (1991) used FQT to show that bovine mitochondrial cytochrome *c* reductase (Complex III) interacted with HOQNO with a K_d close to 50 nM for both reduced and oxidized reductases (Brandt and von Jagow 1991). Other uses of FQT and HOQNO included bacterial respiratory complexes such as the *E. coli* fumarate and DMSO reductases, which have shown to exhibit strong interactions with HOQNO, K_d of 2.5 and 7.1 nM, respectively (Geijer and Weiner 2004; Rothery et al. 2005). These data were also determined using membrane preparations expressing complete oxidoreductases DmsABC or FrdABCD and not purified protein. It is possible that HOQNO-CymA interactions would be greater when CymA is expressed as a complex with a terminal reductase such as arsenate respiratory reductase (e.g., ArrAB in *Shewanella*).

Because HOQNO is non-redox active, we used the redox active menaquinol analog $DMNH_2$ to show that CymA can be reduced by a model MQH_2 substrate (Fig. 4). Similarly to HOQNO, $DMNH_2$ has been used to probe the redox properties of DmsABC and FrdABCD, for example (Geijer and Weiner 2004). Our observations provide a basis to test the hypothesis that CymA functions as a quinol-oxidase that can reduce ArrAB. Further biochemical investigations will be required to determine the kinetic properties of reduction and oxidation when CymA is part of a terminal reductase complex.

Based on multiple sequence alignments with NrfH and protein structure modeling, we identified a lysine residue (Lys91) in the second helix of CymA that is predicted to be important for binding MQH_2 (Fig. 2b). Changing Lys91 (a positively charged residue) to Gln (a polar, uncharged group with similar side chain length) disrupted CymA interactions with MQH_2 substrates. Through FQT with HOQNO and MQH_2-CymA reduction experiments, we showed that the CymA-K91Q MQH_2 interactions and heme reduction were significantly diminished (Figs. 3, 4). A K_d for HOQNO with CymA-K91Q could not be determined because of the nearly linear response of HOQNO titration into membrane preparations enriched in CymA-K91Q. The critical role of Lys91 in MQH_2-CymA interaction is supported by molecular modeling of the *D. vulgaris* NrfH docked with HOQNO showing that Lys82 (Lys91 in CymA) forms an H-bond with the *N*-oxide

(replacing one of the carbonyl groups) of HOQNO, helping to keep it in place (Rodrigues et al. 2006; 2008). The K91Q alteration in CymA most likely disrupted one of the H-bonds necessary for the interaction of HOQNO with CymA, resulting in weakened interaction with HOQNO and the near linear FQT response (Fig. 3c). The lack of growth on arsenate (fumarate and Fe(III) citrate) for pAN-*cymA*-K91Q (Fig. 5, Fig. S1B) provides further evidence in support of Lys91 as a critical residue for MQH_2 oxidation and heme reduction of CymA. We also investigated Lys90 because of its close proximity to Lys91. Neither NrfH nor NapC has this second proximal Lys residue. Growth curve analysis of *cymA*-K90Q allele in *Shewanella* sp. ANA-3 Δ*cymA* strain was indistinguishable from the wild type indicating that Lys90 might not be important for MQH_2 interaction. Based on the CymA homology model, there are likely other amino acid residues in CymA that are involved in MQH_2 interactions and heme reduction (Fig. 2b, e.g., K96, D97).

The homology model of CymA (Fig. 2b) indicates that helix 2 (H2) amino acid residues might be responsible for the interaction with menaquinol. Schwalb et al. (2003) provided biological evidence that a soluble form of CymA (missing the first 35 amino acids comprising the N-terminal helix, helix 1) was functional because it could reduce the soluble fumarate reductase flavocytochrome FccA (Schwalb et al. 2003). Furthermore, it was shown that the soluble version of CymA could complement a *cymA* disruption mutant in MR-1. This indicated that even though the membrane-anchoring helix (H1) could be removed, CymA might still have the capacity to associate with the cytoplasmic membrane through the second helix, and that H2 amino acid residues might be sufficient for menaquinol interaction and oxidation.

Our data support the hypothesis that CymA is the electron mediator between the menaquinol pool and the arsenate respiratory reductase (ArrAB). Because CymA has four low-spin hemes with redox potentials of +10, −108, −136, and −229 mV, menaquinols (E_o' −74 mV) would be preferred over ubiquinols (E_o' +112 mV) (Field et al. 2000) as reductants for arsenate reduction (electrochemical potential E_o' As(III)/As(V) = +139 mV). Furthermore, CymA shares homology with other NapC/NrfH *c*-type tetraheme cytochromes in that a lysine residue on the second helix is important for menaquinol interaction, electron transfer, and/or possibly proton translocation (Roldan et al. 1998). Lastly, in *Shewanella* (ANA-3 and other strains), CymA has an interesting physiological function because it acts as a major branching point to other electron transport chains including arsenate, DMSO, fumarate, nitrate, nitrite, vanadate, and oxides of Fe(III) and Mn(IV) (Myers and Myers 1997; Schwalb et al. 2002; Myers et al. 2004; Murphy and Saltikov 2007). Compared to the nitrite reductase complex of *D. vulgaris*, which consists of NrfA (α) and NrfH (β) in a $\alpha_4\beta_2$ configuration, it is still unclear whether CymA forms a multimeric complex with itself or other proteins (Rodrigues et al. 2006). Further investigations of the interaction of CymA and ArrAB will be insightful for understanding the details of the electron transport chain leading to arsenate reduction and other electron acceptors in *Shewanella* species.

Acknowledgments We thank Professor Gary Cecchini and Dr. Elena Maklashina (University of California, San Francisco) for helpful discussion on FQT data analysis and Professor Ming Tien (Pennsylvania State University, University Park) and colleagues for providing pEC86. We also like to thank Professor Theodore Holman and his laboratory members for insightful discussions and the use of the fluorescence spectrometer. Funding was provided by the National Science Foundation, Research Starter Grant, MCB-0731276.

References

Arnold K, Bordoli L, Kopp J, Schwede T (2006) The SWISS-MODEL workspace: a web-based environment for protein structure homology modelling. Bioinformatics 22:195–201

Berry EA, Trumpower BL (1987) Simultaneous determination of hemes a, b, and c from pyridine hemochrome spectra. Anal Biochem 161:1–15

Brandt U, von Jagow G (1991) Analysis of inhibitor binding to the mitochondrial cytochrome c reductase by fluorescence quench titration. Evidence for a 'catalytic switch' at the Qo center. Eur J Biochem 195:163–170

Campbell KM, Malasarn D, Saltikov CW, Newman DK, Hering JG (2006) Simultaneous microbial reduction of iron(III) and arsenic(V) in suspensions of hydrous ferric oxide. Environ Sci Technol 40:5950–5955

Field SJ, Dobbin PS, Cheesman MR, Watmough NJ, Thomson AJ, Richardson DJ (2000) Purification and magneto-optical spectroscopic characterization of cytoplasmic membrane and outer membrane multiheme c-type cytochromes from *Shewanella frigidimarina* NCIMB400. J Biol Chem 275:8515–8522

Francis RT Jr, Becker RR (1984) Specific indication of hemoproteins in polyacrylamide gels using a double-staining process. Anal Biochem 136:509–514

Geijer P, Weiner JH (2004) Glutamate 87 is important for menaquinol binding in DmsC of the DMSO reductase (DmsABC) from *Escherichia coli*. Biochimica Et Biophysica Acta-Biomembranes 1660:66–74

Jones DT (1999) Protein secondary structure prediction based on position-specific scoring matrices. J Mol Biol 292:195–202

Kovach ME, Phillips RW, Elzer PH, Roop RM, Peterson KM (1994) pBBR1MCS—a broad-host-range cloning vector. Biotechniques 16:800

Lancaster CR et al (2000) Essential role of Glu-C66 for menaquinol oxidation indicates transmembrane electrochemical potential generation by Wolinella succinogenes fumarate reductase. Proc Natl Acad Sci USA 97:13051–13056

Murphy JN, Saltikov CW (2007) The cymA gene, encoding a tetraheme c-type cytochrome, is required for arsenate respiration in *Shewanella* species. J Bacteriol 189:2283–2290

Myers CR, Myers JM (1997) Cloning and sequence of *cymA*, a gene encoding a tetraheme cytochrome *c* required for reduction of iron(III), fumarate, and nitrate by *Shewanella putrefaciens* MR-1. J Bacteriol 179:1143–1152

Myers JM, Antholine WE, Myers CR (2004) Vanadium(V) reduction by *Shewanella oneidensis* MR-1 requires menaquinone and cytochromes from the cytoplasmic and outer membranes. Appl Environ Microbiol 70:1405–1412

Oremland RS, Stolz JF (2003) The ecology of arsenic. Science 300:939–944

Reyes C, Lloyd JR, Saltikov CW (2008) Geomicrobiology of iron and arsenic in anoxic sediments. In: Ahuja S (ed) Arsenic contamination of groundwater: mechanisms, analysis, and remediation. Wiley, Hoboken, pp 123–146

Rodrigues ML, Oliveira TF, Pereira IA, Archer M (2006) X-ray structure of the membrane-bound cytochrome c quinol dehydrogenase NrfH reveals novel haem coordination. EMBO J 25:5951–5960

Rodrigues ML, Scott KA, Sansom MS, Pereira IA, Archer M (2008) Quinol oxidation by c-type cytochromes: structural characterization of the menaquinol binding site of NrfHA. J Mol Biol 381:341–350

Roldan MD et al (1998) Spectroscopic characterization of a novel multiheme c-type cytochrome widely implicated in bacterial electron transport. J Biol Chem 273:28785–28790

Rothery RA, Weiner JH (1996) Interaction of an engineered [3Fe-4S] cluster with a menaquinol binding site of *Escherichia coli* DMSO reductase. Biochemistry 35:3247–3257

Rothery RA et al (2005) Defining the Q-site of *Escherichia coli* fumarate reductase by site-directed mutagenesis, fluorescence quench titrations and EPR spectroscopy. Febs J 272:313–326

Saltikov CW, Newman DK (2003) Genetic identification of a respiratory arsenate reductase. Proc Natl Acad Sci USA 100:10983–10988

Saltikov CW, Cifuentes A, Venkateswaran K, Newman DK (2003) The *ars* detoxification system is advantageous but not required for As(V)-respiration by the genetically tractable *Shewanella* species, strain ANA-3. Appl Environ Microbiol 69:2800–2809

Saltikov CW, Wildman RA Jr, Newman DK (2005) Expression dynamics of arsenic respiration and detoxification in *Shewanella* sp. Strain ANA-3. J Bacteriol 187:7390–7396

Schwalb C, Chapman SK, Reid GA (2002) The membrane-bound tetrahaem c-type cytochrome CymA interacts directly with the soluble fumarate reductase in *Shewanella*. Biochem Soc Trans 30:658–662

Schwalb C, Chapman SK, Reid GA (2003) The tetraheme cytochrome CymA is required for anaerobic respiration with dimethyl sulfoxide and nitrite in *Shewanella oneidensis*. Biochemistry 42:9491–9497

Thompson JD, Higgins DG, Gibson TJ (1994) CLUSTAL W: improving the sensitivity of progressive multiple sequence alignment through sequence weighting, position-specific gap penalties and weight matrix choice. Nuc Acids 467:3–4680

Thony-Meyer L, Fischer F, Kunzler P, Ritz D, Hennecke H (1995) *Escherichia coli* genes required for cytochrome *c* maturation. J Bacteriol 177:4321–4326

Tufano KJ, Reyes C, Saltikov CW, Fendorf S (2008) Reductive processes controlling arsenic retention: revealing the relative importance of iron and arsenic reduction. Environ Sci Technol 42:8283–8289